Sensors and Actuators B 267 (2018) 224–230

Contents lists available at ScienceDirect

Sensors and Actuators B: Chemical

journal homepage: www.elsevier.com/locate/snb

Bioinspired detection sensor based on functional nanostructures of S-proteins to target the folate receptors in breast cancer cells

Samar Damiati[a,b,*], Martin Peacock[c], Rami Mhanna[d], Sindre Søpstad[c,e], Uwe B. Sleytr[f], Bernhard Schuster[b]

[a] Department of Biochemistry, Faculty of Science, King Abdulaziz University (KAU), Jeddah, Saudi Arabia
[b] Institute for Synthetic Bioarchitectures, Department of Nanobiotechnology, University of Natural Resources and Life Sciences (BOKU), Vienna, Austria
[c] Zimmer and Peacock Ltd, Royston SG8 9JL, UK
[d] Biomedical Engineering Program, American University of Beirut, Beirut, Lebanon
[e] Department of Microsystems, Faculty of Maritime and Natural Sciences, University College of Southeast Norway, Borre, Norway
[f] Institute for Biophysics, Department of Nanobiotechnology, University of Natural Resources and Life Sciences (BOKU), Vienna, Austria

ARTICLE INFO

Article history:
Received 22 September 2017
Received in revised form 27 February 2018
Accepted 7 April 2018
Available online 9 April 2018

Keywords:
Bioinspired materials
S-layer proteins
Acoustic biosensors
Folate receptors
Breast cancer

ABSTRACT

Development of biosensors requires a well-organized template to enhance the sensing specificity. Biological molecules that have the ability to self-assemble into ordered structures can be exploited to construct nanostructures and nanodevices. In this regard, bacterial surface layer proteins (SbpA) have been used as an underlying matrix to bind molecules on the nanometer scale. The present study provides evidence that a gold substrate functionalized with folate-modified SbpA can be used as a sensor for breast cancer cells with superior efficacy over traditional sensors. The developed sensor uses folate to recognize folate receptors, which are highly expressed on the cell membranes of some cancer cells, such as breast cancer cells. To examine the specificity of the developed sensor, folate was used as a binding partner for folate receptors on breast cancer cells (MCF-7), and liver cancer cells (HepG2) were used as the control because they lack folate receptors. The fabricated biosensor comprised a gold surface and a recrystallized S-layer protein lattice functionalized with folate and addressed acoustically and electrochemically. Acoustic studies performed using quartz crystal microbalance with dissipation monitoring (QCM-D) showed the efficiency of the developed biosensor in distinguishing between MCF-7 and HepG2 cells. Despite the ability of QCM-D to recognize cells in situ and in real-time, this biosensor had a limited detection range (1×10^5 cells/mL). To confirm the functionality of the developed platform, electrochemical measurements were performed and the obtained results were in agreement with the acoustic sensor and proving the efficiency of the designed sensing layer. The S-layer lattice-folate modified biosensor provides a promising strategy for designing efficient sensing platforms that can be used to diagnose early stage cancers with highly expressed folate receptors.

1. Introduction

Breast cancer is the most common cancer in women in developed and developing countries, and its distant metastases are the major cause of breast cancer mortality [1,2]. According to the World Health Organization (WHO), more than 508,000 women diagnosed with breast cancer died in 2011. Lower survival rates are largely found in less developed countries, where most cases are diagnosed in late stages because of a lack of effective diagnostic and treatment strategies. Hence, the development of early detection and quantification techniques for breast cancer is important for improving treatment and lowering the mortality rate.

The key to developing a diagnostic biosensor with good biocompatibility for the efficient recognition and capture of target cancer cells is the interface matrix. Several studies have reported the use of polymers, peptides, or gold nanoparticles to modify the sensor surface and to enhance the capturing characteristics of the fabricated immunosensors [3–6]. Furthermore, self-assembled protein nanostructures can be exploited as promising biomaterials to develop functional sensors for diagnostic and pharmaceutical applications [7–10]. Bacterial surface layer (S-layer) proteins are two-dimensional arrays of proteinaceous subunits that form the outermost cell envelope structure on almost all archaea and bacteria [11–14]. The thickness of the S-layers is up to 70 nm in archaea and 5–10 nm in bacteria, and most S-lattices are composed of a sin-

* Corresponding author at: Department of Biochemistry, Faculty of Science, King Abdulaziz University (KAU), Jeddah, Saudi Arabia.
E-mail address: sdamiati@kau.edu.sa (S. Damiati).

https://doi.org/10.1016/j.snb.2018.04.037
0925-4005/

gle protein or glycoprotein with a molecular weight in the range of 40–200 kDa. The subunits of the S-layer protein are aligned in oblique, square, or hexagonal lattice symmetries and have center-to-center spacing of approximately 5–30 nm. Moreover, S-layer proteins exhibit a precise arrangement of functional binding groups and pores of identical size and morphology with diameters ranging between 2–8 nm [12–16]. S-layer proteins can assemble into monomolecular lattices in suspensions and on different solid substrates, such as gold, silicon and phospholipid films [12,17–20]. Thus, S-lattice has been exploited as an effective matrix in many applications, including biosensing and biomimetic platforms for peptide/protein studies [7,21,22].

Current cancer diagnostic techniques, such as flow cytometry, polymerase chain reaction (PCR), immunofluorescence and immunohistochemistry, have the advantage of being well established means of monitoring cell viability and proliferation [23,24]. However, these conventional methods have limited cell detection and are costly, time-consuming and labor intensive [3,25,26]. Recently, a quartz crystal microbalance with dissipation monitoring (QCM-D) has attracted considerable attention in cancer research, but it is still in the development phase. QCM-D is a real-time and label-free technique that determines the kinetics of cell attachment, adhesion and spreading on different surface layers [3,27]. This technology is based on acoustic wave propagation along a quartz crystal that measures the shifts in the resonance frequency (Δf) and energy dissipation factor (ΔD), thus allowing for continuous monitoring of an attached mass on the quartz crystal and evaluation of the viscoelastic and mechanical properties of the attached layer [28–30]. Moreover, QCM-D can track the cellular response after exposure to chemotherapeutics and exogenous stimulation with respect to cell viability [31–33]. In contrast to PCR, which detects markers in cell lysates, QCM-D enables detection of the whole/intact cell by recognizing the surface markers on the cell membrane. However, electrochemical methods are widely used in point-of-care (POC) devices, because of their simplicity, rapid analysis, low-cost, and disposability. Electrochemical biosensors can detect disease markers with high selectivity and sensitivity [4,5,26,34–37].

One of the most important factors limiting the selectivity and sensitivity of the currently available biosensors is the orientation and density of the captured antibodies or aptamers on the sensor surface. As a promising alternative targeting strategy, folate receptors have recently been used to detect and capture intact cancer cells. The expression of folate receptors in healthy tissues and organs is limited, but the expression increases in ovarian, breast, lung, epithelial, kidney and brain tumors [38–40]. The present work reports the first fabrication of S-layer lattice-folate-modified acoustic and electrochemical biosensors to detect breast cancer cells (MCF-7). To test the biosensor, a suspension of MCF-7 cells was passed over the modified sensor surface. The recognition of MCF-7 cells was studied in real-time using QCM-D, cyclic voltammetry (CV), and square wave voltammetry (SWV). With these methods, the efficiency of the fabricated biosensors to detect folate receptors was determined. Moreover, to confirm the selectivity for MCF-7 breast cancer cells, the data were compared with data from other cells, such as HepG2 liver cancer cells, which lack folate receptors on their cell surface. The presented strategy has great potential for diagnostic applications in cancer.

2. Experimental section

2.1. Isolation of S-layer proteins

SbpA proteins molecules (MW 127 kDa) were isolated from *Lysinibacillus sphaericus* CCM 2177 according to a previously described protocol [41]. The final protein solution was stored at 4 °C in Milli-Q water.

2.2. Functionalization of S-layer proteins with folate

Because of the poor solubility of folic acid (Sigma), 30 mg was dissolved in 20 mL of Milli-Q water, and 150 μL of NaOH (1 M) (final concentration 1.5 mg/mL) was added. The mixture was stirred at room temperature in the dark until the yellow solution became clear. Then, EDC (10 mM) and NHS (10 mM) were added, and the solution was stirred for approximately 3 min. To prepare the SbpA-folate conjugate, the activated folate solution (375 μL) was added to SbpA solution (1500 μL, 1 mg/mL). The resulting mixture was stirred at room temperature in the dark for 6 h and stored at 4 °C until further use. The conjugate solution was diluted with crystallization buffer (150 mM NaCl, 10 mM HEPES buffer, pH 7.4) at 1:10 before use to prevent self-assembly formation.

2.3. Cell lines and cell culture

Human breast adenocarcinoma cell line (MCF-7) and human liver hepatocellular carcinoma cell line (HepG2) were obtained from the American Type Culture Collection. MCF-7 and HepG2 cells were cultured in DMEM (PAA Laboratories GmbH, Austria) supplemented with insulin (10 μg/mL) and 10% FBS, respectively, and a 1% antibiotic/antimycotic solution. The cells were grown under standard cell culture conditions according to a previously described protocol [22].

2.4. Contact angle measurements

Ten nanometer thick, gold-coated slides were cleaned in a 5:1:1 mixture of Milli-Q water, NH_3 (33%), and H_2O_2 (30%) and then cleaned in a plasma cleaner (Plasma Prep 2, Germany) to remove organic contaminants.

The water contact angles on bare gold chips or on modified layers were obtained using a goniometer (Easy Drop, Krüss, Germany). A 5 μL Milli-Q water drop was deposited on the dried surface, and CA was immediately determined. This experiment was performed at least three times on different positions.

2.5. QCM-D experiments

The gold sensors that were used for this work are commercially available (Q-Sense, Sweden). Before each experiment, the sensors were cleaned in a mixture (5:1:1) of Milli-Q water, NH_3 (33%), and H_2O_2 (30%) at 70 °C for approximately 10 min and a subsequent UV/ozone treatment.

The QCM-D measurements were performed in triplicate at 27 or 37 ± 0.02 °C. The flow rate was either 100 μL min^{-1} or 50 μL min^{-1}. Briefly, a dilute solution of the SbpA – folate mixture was recrystallized on the gold surface overnight at 27 °C and subsequently rinsed with Milli-Q water to remove any excess materials. Afterward, BSA (1%) in PBS was injected and incubated for 60 min. Subsequently, temperature was increased to 37 °C and cancer cells in the PBS solution were injected and incubated for approximately 60 min and then a rinse step with PBS solution was performed to remove unbound cells.

2.6. Electrochemical measurements

The potentiostat (Ana Pot, Zimmer and Peacock Ltd, UK) was used to measure CV and SWV. Electrochemical measurements were performed in $K_3[Fe(CN)_6]$ (10 mM) solution containing KCl (100 mM) at a scan rate of 50 mV/s.

The screen-printed electrodes (Zimmer and Peacock Ltd, UK) were exposed to a solution of SbpA-folate conjugate overnight

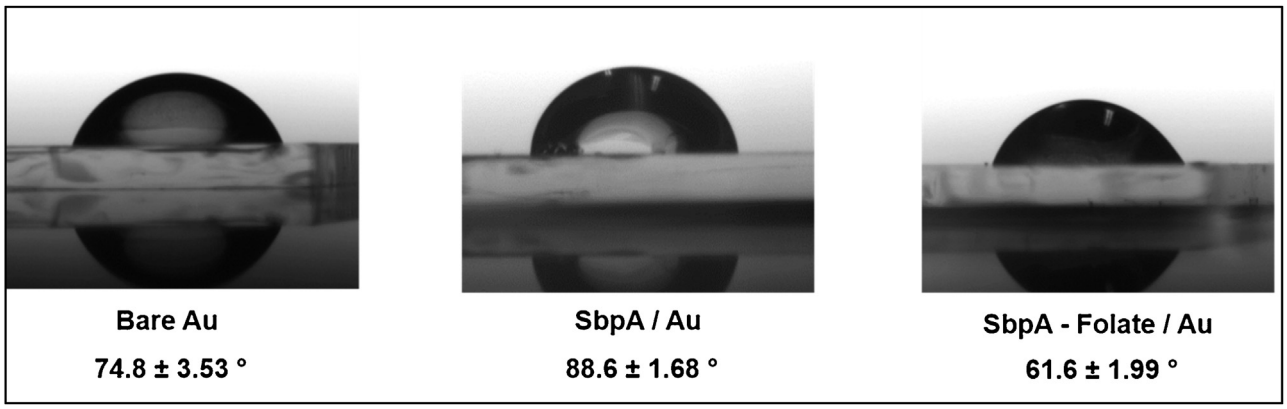

Fig. 1. Water contact angles for bare gold, S-layer protein (SbpA) and functionalized SbpA-folate layers.

at room temperature. After recrystallization of the modified S-layer proteins, the surface was rinsed with crystallization buffer to remove the excess protein. Then, the modified sensors were incubated with different cell densities of the breast or liver cells at 37 °C. In the last step, sensors were rinsed with PBS solution to remove unbound cells.

3. Results and discussion

3.1. Investigation of Au/SbpA-folate modified biosensor biocompatibility: contact angle (CA) measurements

To make a biosensor specific for cancer cells, many studies have fabricated sensors based on the specific recognition of protein receptors that are usually overexpressed on the surface of the cell membrane. In this study, the S-layer lattice was functionalized with folate, the synthetic form of vitamin B9, to detect the folate receptors on MCF-7 breast cancer cells. In general, the recognition and interaction of cells on the fabricated sensors is highly affected by the nature of the sensor surface. Hydrophilicity, wettability, and surface charge are important factors that can influence cell attachment or proliferation [42]. Therefore, the wetting properties of the fabricated sensor were investigated by measuring the CA (Fig. 1). However, the S-layer proteins can form water-filled hydrophilic pores with low, unspecific adsorption, because of their antifouling properties [43]. Charged groups, such as carboxy- or amino-moieties, on the surface of the S-lattice contribute to an increase in surface hydrophilicity [12]. Hence, the SbpA-folate conjugate was formed by reacting folate with SbpA in the presence of EDC and NHS. EDC is a water-soluble carbodiimide and is commonly used to conjugate biological materials containing amines and carboxylates; NHS is usually used in combination with EDC to improve the efficiency by forming amine reactive intermediates [21,44]. In this case, cross-linking leads to a stable amide bond between folate and SbpA molecules.

The CA for the bare gold surface was $74.8 \pm 3.53^{\circ}$ and increased to $88.6 \pm 1.68^{\circ}$ after recrystallization of the SbpA on the gold surface. In contrast, SbpA functionalized with folate showed improved hydrophilicity and thus CA decreased to $61.6 \pm 1.99^{\circ}$, owing to the presence of the hydroxyl and carboxyl groups of the SbpA and folate. This decrease in CA demonstrated that the SbpA-folate layer can provide a biocompatible surface because of its inherent properties that may enhance the cell loading.

3.2. Characterization of the acoustic Au/SbpA-folate modified sensor

QCM-D is a surface-sensitive microbalance technique uses to measure frequency (Δf), which presents the mass of the material adsorbed on or removed from the sensor, and energy dissipation (ΔD), which reports on the energy loss and the viscoelastic properties before, during, and after molecules adsorption [30].

In the present study, QCM-D was used to track the recrystallization of the S-layer protein functionalized with folate on the gold sensors at 27 °C and the binding of cancer cells at 37 °C (Fig. 2). The shifts in the Δf and ΔD signals occurred simultaneously after injection of the SbpA-folate conjugate and after injection of the cancer cells. The self-assembly of the modified SbpA proteins from solution, which formed a lattice on the gold substrate, resulted to a rapid reduction in the frequency signal to approximately −80 Hz and an increase in the energy dissipation level (approximately 25×10^{-6}). After rinsing with water, a significant change in the Δf (approximately 55 Hz) and ΔD (approximately 15×10^{-6}) signals was observed because of the removal of excess protein molecules. In the absence of folate (Fig. S1), the wild-type SbpA lattice had a higher frequency value (>100 Hz) and a lower dissipation value (approximately 2.5×10^{-6}), thus indicating that folate may affect the self-assembly of the S-protein subunits and the formation of a tightly bound, rigid layer on the gold sensor [7,17,45]. In fact, the lower Δf value in combination with the higher ΔD observed for the SbpA-folate conjugate suggests the presence of an incomplete and soft proteinaceous layer on the gold surface.

BSA is usually used as a blocking agent in biosensors to minimize non-specific binding. In principle, because of the antifouling properties of the S-lattice, there is no need to block the surface, but in the present study, BSA was added to block unspecific binding. A slight decrease in the frequency signal (−65.5 Hz) and a noticeable decrease in the dissipation signal (7.5×10^{-6}) were observed after the addition of BSA. The small drop in frequency and drop in dissipation may indicate that BSA molecules were retained within the incomplete SbpA-folate layer making the layer stiffer. These measurements were performed in triplicate and the mean of frequency and dissipation values for the generated layers before and after rinsing steps are presented in Table S1. Subsequently, the system was allowed to equilibrate in PBS for one hour at 37 °C.

3.3. Detection of MCF-7 cells via the fabricated acoustic sensor (Au/SbpA-folate)

A carefully designed surface architecture can improve the efficiency and performance of biosensors. Most available biosensors depend mainly on antibodies/aptamers capturing the target cells. According to literatures, the greatest limitations of these sensors are that the antibodies/aptamers must be precisely oriented, and the fabricated surface must be uniform. Interestingly, the cell capture efficiency significantly improves when the thickness of the sensing layer is decreased and vice versa [46]. The proposed biosen-

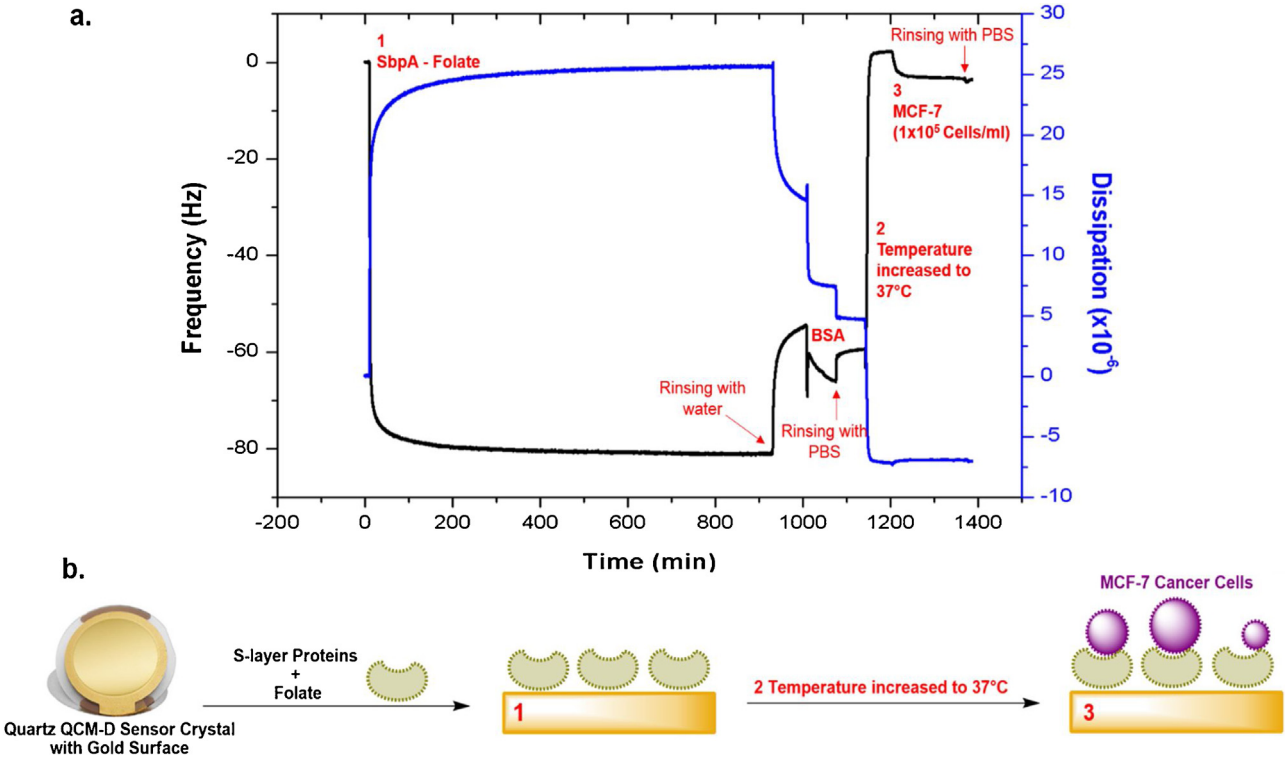

Fig. 2. (a) Representative shift in frequency and dissipation versus time for the formation of the final functionalized SbpA-folate/Au sensor structure and the subsequent addition of MCF-7 cells at concentration 1×10^5 cells/ml. All shown QCM-D data were recorded at the 5th overtone. (b) The schematic sketch (not drawn to scale) shows the step-by-step modification of the gold sensor to the final SbpA-folate/Au sensor surface: (1) recrystallization of the functionalized S-layer protein SbpA modified with folate on the gold sensor; (2) increasing the temperature from 27 °C to 37 °C; (3) specific recognition of MCF-7 breast cancer cells.

sor in this study overcomes these limitations by having a SbpA lattice nanostructure with a small thickness (9 nm) [47]. Moreover, antibody/aptamer immobilization is not a concern, because the SbpA lattice is functionalized with folate to recognize the folate receptors on cancer cells. Finally, an extra antibody layer is not needed, thus further minimizing the thickness of the biosensing layer.

The evaluation of the direct capture of MCF-7 cells on the functionalized QCM-D sensor was performed by tracking the changes in the frequency and dissipation at 3rd to 13th odd-numbered overtones. In principle, the adhesion of cells may result in a completely different Δf shift, because QCM-D also responds to the particle resonance frequency [30]. In brief, the particle resonance frequency depends on not only the adsorbed mass but also the adhesive bond stiffness. Frequency presents negative signal when the cells are tightly immobilized on the sensor surface [3]. When the cell is bind to a long and flexible linker, and the stiffness of the adhesive bonds is low, even a positive shift in Δf can be measured for cell binding by QCM-D [30]. The specific binding of a cell with a short linker results in a shift of Δf in between the two aforementioned boundary conditions. The modified sensors (SbpA-folate on Au) were exposed to a suspensions of MCF-7 cells at different cell densities (1×10^4, 1×10^5, and 5×10^5 cells/mL) to investigate the sensitivity of the biosensor (Figs. 2 and 3a. The results showed that the Δf and ΔD signals were dependent on cells densities, but the changes in the signals was not considerable at low cell densities. This result indicated that the limit of detection for the fabricated sensor is $\sim 1 \times 10^5$ cells. However, several published studies have shown a significant change in the mass adsorbed on the surface when the cells were directly attached to the surface [3,48,49]. In contrast, in the present work, the intermediate SbpA-folate layer resulted in a space between the cancer cells and the gold surface, and the measured changes in the frequency were smaller. To confirm the reproducibility of the developed system, experiments were repeated and frequency results were summarized in Table S2. Furthermore, two important findings were observed when QCM-D was used to detect cancer cells. First, the temperature must be optimized (increased from 27 to 37 °C) to achieve efficient cell capture on the fabricated biosensor. Second, QCM-D can distinguish between viable and non-viable cells in real-time. The QCM-D measurements were carried out when the cell viability levels were approximately 90% and 10% (Fig. 3a and b). When the viable cells were exposed to the fabricated sensor, the frequency signals changed significantly, thus indicating the binding interaction between the folate and the folate receptors on MCF-7 cells. In contrast, the non-viable cells did not show significant changes in the frequency signals, thus indicating that no mass had adsorbed on the sensing surface. These observations were consistent with findings from our previous work [18].

3.4. *Characterization of the electrochemical Au/SbpA-folate modified sensor and detection of MCF-7 cells*

One of the most common cancer diagnostic methods is PCR. In this technique, mRNA is first extracted, and marker detection is performed on the cell lysate. This study sought to find a simpler approach by detecting whole/intact cells, by using techniques such as QCM-D, as described above, and electrochemistry. Hence, electrochemical methods were used to confirm the efficiency of the fabricated acoustic sensor. The fabricated SbpA-folate coated gold electrode was characterized using CV measurements and all electrochemical measurements were conducted in 10 mM $[Fe(CN)_6]^{3-}$ solution containing 100 mM KCl (Fig. 4). The bare gold surface showed the highest peak current, thus indicating a small resistance in the electron transfer. After recrystallization of SbpA on the gold electrode, the peak current decreased from 115.20 μA to

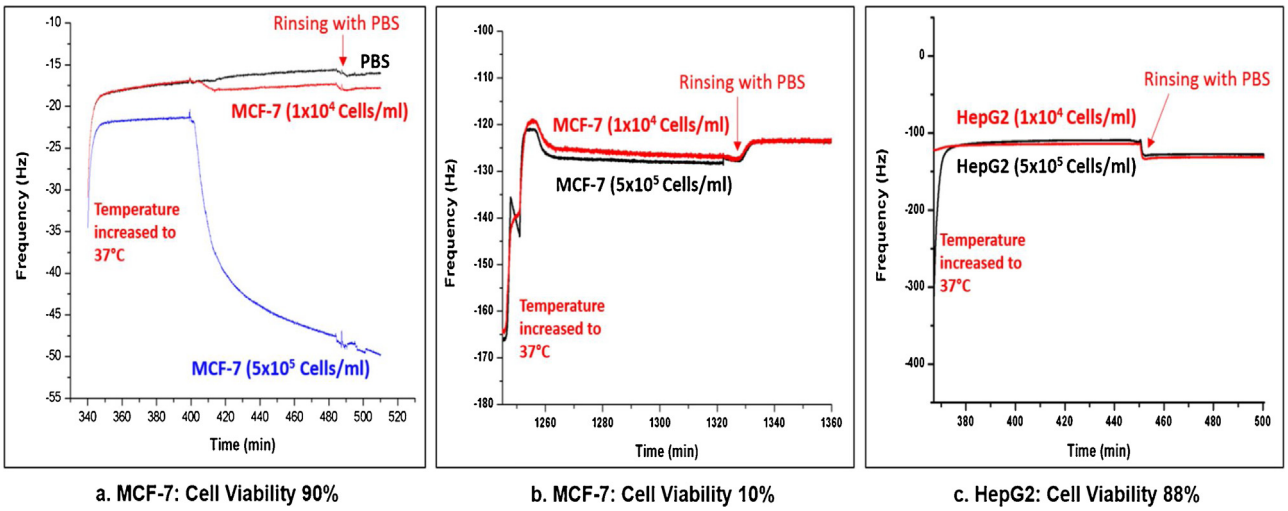

Fig. 3. Frequency shifts recorded at the 5th overtone as function of time for the capturing of cancer cells by the functionalized SbpA-folate/Au QCM-D-sensor at two different concentrations (1×10^4 and 5×10^5 cells/ml), (a) capturing of MCF-7 breast cancer cells (cell viability 90%), (b) capturing of MCF-7 breast cancer cells (cell viability 10%), and **(c)** capturing of HepG2 liver cancer cells (cell viability 88%).

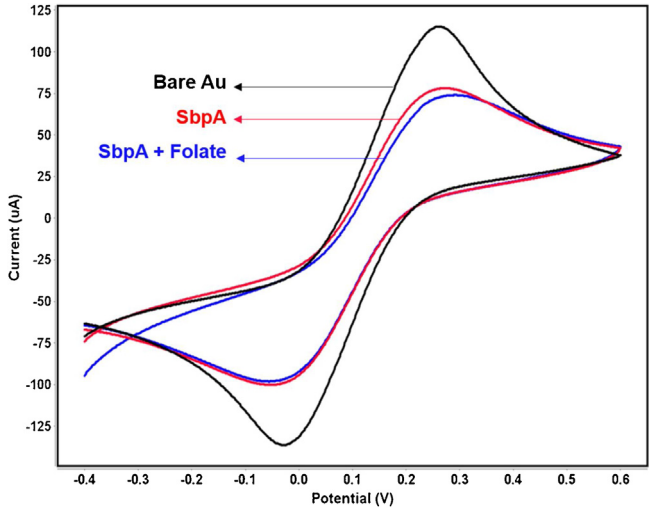

Fig. 4. CV spectra of the bare gold electrode and S-lattice with or without folate on gold electrode in 10 mM $K_3[Fe(CN)_6]$ containing 100 mM KCl at a scan rate of 50 mV/s.

77.60 μA (without folate) and 75.54 μA (with folate), thus reflecting a decrease in the electron transfer resistance. These changes in the electrochemical properties at each layer indicated successful modifications of the functionalized electrode.

After modification of the gold electrode with the SbpA-folate, a suspension of MCF-7 cells was added to the developed sensor at different cell densities, and SWV measurements were performed in absence (no cells) and presence of cancer cells. Because of the specific interaction between the folate bound on the surface and the folate receptors, which are overexpressed by breast cancer cells, the ability of the fabricated biosensor to capture MCF-7 cells was verified (Fig. 5a). Generally, when SWV measurements are performed, increasing the analyte concentration increases the current response. However, in this study, the SWV measurements converted the interaction between the folate and the folate receptors on MCF-7 cancer cells into an electrical signal. The SWV was measured for the increasing MCF-7 cell densities (1×10^4, 1×10^5, and 5×10^5 cells/mL) and compared to a blank test (no cells). The peak current consistently increased (65, 108, and 185 μA, respectively) with an increasing number of cells captured on the sensor surface, as compared to the initial value with no cells (18 μA). This increase indicated higher coverage of the electrode surface by the captured cells. It is evident from the obtained results that there is a dependency between cell count and current magnitude. However, instead of the inverse proportionality expected by an increasing electrode coverage, the signal is in fact increasing. Although this appears counterintuitive to the expected result, it could be attributed to that of a succeeding catalytic electrochemical reaction mechanism (EC'): After having passed through the biolayers on the electrode, $[Fe_3(CN)_6]^{3-}$ is reduced to $[Fe_3(CN)_6]^{4-}$ by the working electrode, after which it is immediately reoxidized and ready to once again be reduced by the electrode. This recycling of redox species is an effect which has been previously advantageously utilized in enzymatic disposable glucose strips to further enhance the clinical signal [50]. Human cells are rich in enzymes, which may act as catalysts for the reoxidation of $[Fe_3(CN)_6]^{3-}$. However, these results demonstrated the successful development of an efficient, low-cost and disposable biosensor for the detection of breast cancer cells.

3.5. Selectivity of the SbpA-folate modified sensors for the detection of folate receptors

As mentioned above, selectivity and specificity are critical points that must be considered during biosensor development for cancer cell detection. Hence, QCM-D and SWV were used to characterize the specificity of the SbpA-folate modified electrode for MCF-7 breast cancer cells. The SWV measurements confirmed that this fabricated biosensor was able to efficiently distinguish between breast and liver cancer cells (Fig. 5b). The comparison of the current peaks indicated the high specificity of the SbpA-folate biosensor for MCF-7. Given that HepG2 liver cancer cells do not express folate receptors, these cells cannot bind to the folate on the modified electrode. Although the non-specific adsorption of HepG2 cells may slightly change the electrochemical signals, the significant change in the current peak for MCF-7 breast cells confirms the high selectivity and accuracy of the proposed electrode toward folate receptors for breast cancer detection. These observations are in agreement with QCM-D results in Fig. 3c which shows that the frequency signals were almost unchanged when the sensor was exposed to HepG2 cells at different cell densities (1×10^4 and 5×10^5 cells/mL), thus indicating that no mass had increased on the sensor and hepatic cells were not detectable by the modified surface.

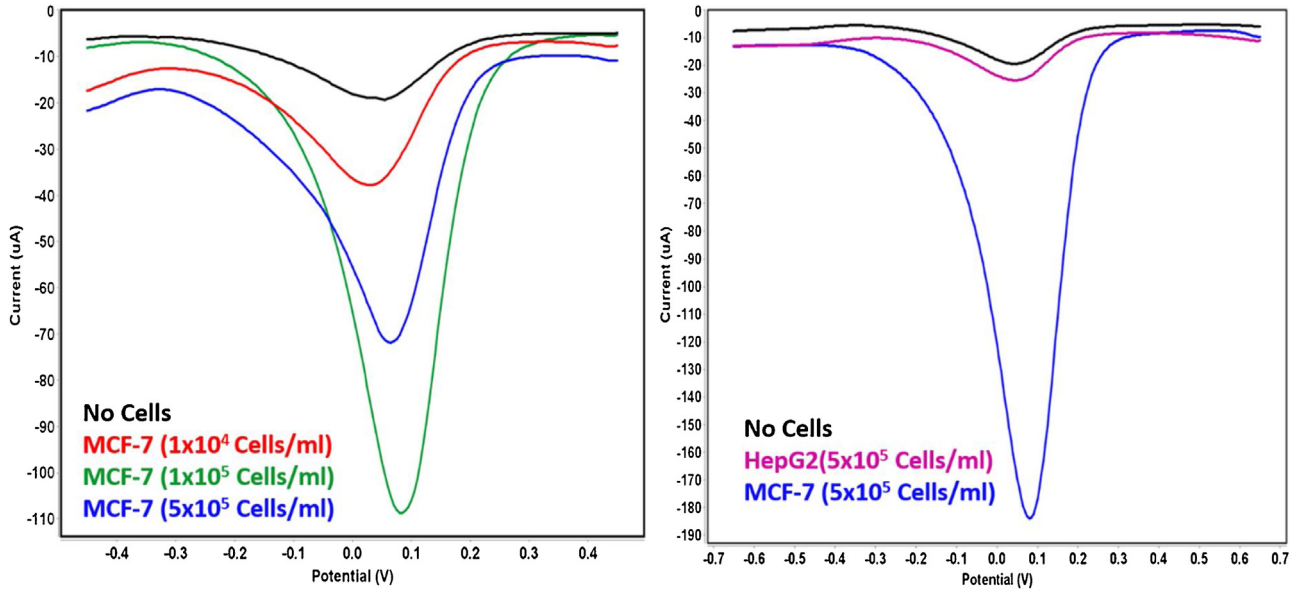

Fig. 5. (a) Square wave voltammograms for MCF-7 breast cancer cells captured on the modified SbpA-folate/Au electrode at different concentrations and (b) Square wave voltammograms for detection of MCF-7 and HepG2 cancer cells at concentration 5×10^5 cells/ml.

4. Conclusion

The present study is the first to conjugate the S-layer protein, SbpA, with folate to functionalize a gold surface for the specific capture of MCF-7 cells through the detection of folate receptors expressed on the surface of breast cancer cells. The fabricated acoustic and electrochemical sensors were able to distinguish between MCF-7 and HepG2 cancer cells because the latter do not express folate receptors. The proposed biosensor offers several advantages that increase the cell capturing efficiency, including the small thickness and the antifouling properties of the S-layer lattice. In addition, antibody/aptamer immobilization is not a concern, because folate can be used as an alternative to antibody/aptamer for detecting target cells. Overall, the evaluation of the developed biosensor by using different techniques provided more information about the efficiency of the system. The QCM-D measurements efficiently tracked the formation of the SbpA-folate modified sensor and the capture of cancer cells in real-time under controlled conditions. Although the QCM-D technique has a limited detection range, it allows for cell viability tracking. Hence, the cellular response to chemotherapeutic agents is worth investigating in future QCM-D studies by analyzing cell numbers change in response to drugs. Importantly, the electrochemical measurements confirmed the selectivity and specificity of the developed biosensor, and thus this method provides a simple, rapid, cost effective and disposable platform for cancer detection. Moreover, the development of efficient biosensors with high selectivity and sensitivity for accurate diagnoses should aid in increasing the remission and survival rates of cancer patients.

Acknowledgements

The authors would like to thank Dr. Seta Küpcü, Institute for Synthetic Bioarcheticture, - Department of Nanobiotechnology (DNBT), University of Natural Resources and Life Sciences (BOKU), Vienna – Austria for her assistance with cell culture, and Dr. Gary Dorken, Institute for Biologically inspired materials, DNBT, BOKU, Vienna – Austria for his assistance with contact angle measurements. Financial support provided from the Austrian Science Fund (FWF), project P 29399-B22 (to B.S.) is gratefully acknowledged.

Appendix A. Supplementary data

Supplementary data associated with this article can be found, in the online version, at https://doi.org/10.1016/j.snb.2018.04.037.

References

[1] A. Amadori, E. Rossi, R. Zamarchi, P. Carli, D. Pastorelli, A. Jirillo, Circulating and disseminated tumor cells in the clinical management of breast cancer patients: unanswered questions, Oncology 76 (2009) 375–386.
[2] J. Benson, I. Jatoi, The global breast cancer burden, Future Oncol. 8 (2012) 697–702.
[3] S. Zhang, H. Bai, J. Luo, P. Yang, J. Cai, A recyclable chitosan-based QCM biosensor for sensitive and selective detection of breast cancer cells in real time, Analyst 139 (2014) 6259.
[4] J. Castillo, S. Gaspar, S. Leth, M. Niculescu, A. Mortari, I. Bontidean, V. Soukharev, S. Dorneanu, A. Ryabov, E. Csoregi, Biosensors for life quality: design, development and applications, Sens. Actuators B 102 (2004) 179–194.
[5] S. Arya, K. Wang, C. Wong, A. Abdur Rahman, Anti-EpCAM modified LC-SPDP monolayer on gold microelectrode based electrochemical biosensor for MCF-7 cells detection, Biosens. Bioelectron. 41 (2013) 446–451.
[6] T. Zheng, R. Zhang, L. Zou, J. Zhu, A label-free cytosensor for the enhanced electrochemical detection of cancer cells using polydopamine-coated carbon nanotubes, Analyst 137 (2012) 1316–1318.
[7] S. Damiati, S. Zayni, A. Schrems, E. Kiene, U. Sleytr, J. Chopineau, B. Schuster, E.-K. Sinner, Inspired and stabilized by nature: ribosomal synthesis of the human voltage gated ion channel (VDAC) into 2D-protein-tethered lipid interfaces, Biomater. Sci. 3 (2015) 1406–1413.
[8] E.M. Egelseer, N. Ilk, D. Pum, P. Messner, C. Schäffer, B. Schuster, U.B. Sleytr, S-Layers, microbial, biotechnological applications, in: M.C. Flickinger (Ed.), Encyclopedia of Industrial Biotechnology: Bioprocess, Bioseparation, and Cell Technology, Wiley, Weinheim Germany, 2010, pp. 4424–4448.
[9] D. Pum, U.B. Sleytr, Reassembly of S-layer proteins, Nanotechnology 25 (2014) 312001.
[10] D. Pum, J.L. Toca-Herrera, U.B. Sleytr, S-layer protein self-assembly, Int. J. Mol. Sci. 14 (2) (2013) 2484–2501.
[11] U.B. Sleytr, T.J. Beveridge, Bacterial S-layers, Trends Microbiol. 7 (6) (1999) 253–260.
[12] U.B. Sleytr, B. Schuster, E. Egelseer, D. Pum, S-layers: principles and applications, FEMS Microbiol. Rev. 38 (2014) 823–864.
[13] U.B. Sleytr, Heterologous reattachment of regular arrays of glycoproteins on bacterial surfaces, Nature 257 (1975) 400–402.
[14] U.B. Sleytr, D. Pum, E. Egelseer, N. Ilk, B. Schuster, S-layer proteins, in: W. Knoll (Ed.), Handbook of Biofunctional Surface, Pan Stanford Publishing, Singapore, 2013, pp. 507–568.
[15] B. Schuster, U.B. Sleytr, Nanotechnology with S-layer proteins, in: J.A. Gerrard (Ed.), Protein Nanotechnology, Humana Press, Totowa, NJ, USA, 2013, pp. 153–157.
[16] N. Ilk, E.M. Egelseer, U.B. Sleytr, S-layer fusion proteins – construction principles and applications, Curr. Opin. Biotech. 22 (2011) 824–831.

[17] B. Schuster, E. Györvary, D. Pum, U.B. Sleytr, Nanotechnology with S-layer proteins, in: T. Vo-Dinh (Ed.), Protein Nanotechnology: Protocols, Instrumentation and Applications; Book Series: Methods in Molecular Biology, Vol. 300, Humana Press, Totowa, NJ, USA, 2005, pp. 101–124.
[18] B. Schuster, D. Pum, M. Sára, U.B. Sleytr, S-layer proteins as key components of a versatile molecular construction kit for biomedical nanotechnology, Mini Rev. Med. Chem. 6 (2006) 909–920.
[19] U.B. Sleytr, B. Schuster, E.M. Egelseer, D. Pum, C.M. Horejs, R. Tscheliessnig, N. Ilk, Nanotechnology with S-layer proteins as building blocks, Prog. Mol. Biol. Transl. Sci. 103 (2010) 277–352.
[20] B. Schuster, U.B. Sleytr, Composite S-layer lipid structures, J. Struct. Biol. 168 (2009) 207–216.
[21] S. Damiati, A. Schrems, E.-K. Sinner, U. Sleytr, B. Schuster, Probing peptide and protein insertion in a biomimetic S-layer supported lipid membrane platform, Int. J. Mol. Sci. 16 (2015) 2824–2838.
[22] S. Damiati, S. Küpcü, M. Peacock, C. Eilenberger, M. Zamzami, I. Qadri, H. Choudhry, U. Sleytr, B. Schuster, Acoustic and hybrid 3D-printed electrochemical biosensors for the real-time immunodetection of liver cancer cells (HepG2), Biosens. Bioelectron. 94 (2017) 500–506.
[23] S.K. Singh, C. Hawkins, I.D. Clarke, J.A. Squire, J. Bayani, T. Hide, R.M. Henkelman, M.D. Cusimano, P.B. Dirks, Identification of human brain tumour initiating cells, Nature 432 (2004) 396–401.
[24] N. Berois, M. Varangot, C. Sonora, L. Zarantonelli, C. Pressa, R. Lavina, J. Rodriguez, F. Delgado, N. Porchet, J. Aubert, E. Osinaga, Detection of bone marrow-disseminated breast cancer cells using an RT-PCR assay of MUC5B mRNA, Int. J. Cancer 103 (2003) 550–555.
[25] M. Miller, G. Doyle, L. Terstappen, Significance of circulating tumor cells detected by the cell search system in patients with metastatic breast colorectal and prostate cancer, J. Oncol. 2010 (2010).
[26] Y. Zhu, P. Chandra, Y. Shim, Ultrasensitive and selective electrochemical diagnosis of breast cancer based on a hydrazine-Au nanoparticle-aptamer bioconjugate, Anal. Chem. 85 (2013) 1058–1064.
[27] L. Tan, X. Jia, X. Jiang, Y. Zhang, H. Tan, S. Yao, Q. Xie, Real-time monitoring of the cell agglutination process with a quartz crystal microbalance, Anal. Biochem. 383 (2008) 130–136.
[28] M. Rodahl, F. Höök, A. Krozer, P. Brzezinski, B. Kasemo, Quartz crystal microbalance set up for frequency and Q-factor measurements in gaseous and liquids environments, Rev. Sci. Inst. 66 (1995) 3924–3930.
[29] C. Fredriksson, S. Kihlman, M. Rodahl, B. Kasemo, The piezoelectric quartz crystal mass and dissipation sensor: a means of studying cell adhesion, Langmuir 14 (1998) 248–251.
[30] A. Olsson, H. Van der Mei, H. Busscher, P. Sharma, Influence of cell surface appendages on the bacterium-substratum interface measured real-time using QCM-D, Langmuir 25 (3) (2009) 1627–1632.
[31] K. Marx, T. Zhou, A. Montrone, D. McIntosh, S. Braunhut, A comparative study of the cytoskeleton binding drugs nocodazole and taxol with a mammalian cell quartz crystal microbalance biosensor: different dynamic responses and energy dissipation effects, Anal. Biochem. 361 (2007) 77–92.
[32] M. Tarantola, E. Sunnick, D. Schneider, A. Marel, A. Kunze, A. Janshoff, Dynamic changes of acoustic load and complex impedance as reporters for the cytotoxicity of small molecule inhibitors, Chem. Res. Toxicol. 24 (2011) 1494–1506.
[33] J. Iturri, L. García-Fernandez, U. Reuning, A. García, A. Campo, M. Salierno, Synchronized cell attachment triggered by photo-activatable adhesive ligands allows QCM-based detection of early integrin binding, Sci. Rep. 5 (2015) 9533.
[34] T. Li, Q. Fan, T. Liu, X. Zhu, J. Zhao, G. Li, Detection of breast cancer cells specially and accurately by an electrochemical method, Biosens. Bioelectron. 25 (12) (2010) 2686–2689.
[35] S. Damiati, M. Peacock, S. Leonhardt, L. Damiati, M.A. Baghdadi, H. Becker, R. Kodzius, B. Schuster, Embedded disposable functionalized electrochemical biosensor with a 3D-printed flow cell for detection of hepatic oval cells (HOCs), Genes 9 (2018) 89.
[36] C. Haslam, S. Damiati, T. Whitley, P. Davey, E. Ifeachor, S.A. Awan, Label-free Sensors based on graphene field-effect transistors for the detection of human chorionic gonadotropin cancer risk biomarker, Diagnostics 8 (2018) 5.
[37] K. Islam, S. Damiati, J. Sethi, A. Suhail, G. Pan, Development of a label-free immunosensor for clusterin detection as an Alzheimer's biomarker, Sensors 18 (2018) 308.
[38] S. Weitman, R. Lark, L. Coney, D. Fort, V. Frasca, V. Zurawski, B. Kamen, Distribution of the folate receptor GP38 in normal and malignant cell lines and tissues, Cancer Res. 52 (12) (1992) 3396–3401.
[39] F. Esmaeili, M.H. Ghahremani, S.N. Ostad, F. Atyabi, M. Seyedabadi, M.R. Malekshahi, M. Amini, R. Dinarvand, Folate-receptor-targeted delivery of docetaxel nanoparticles prepared by PLGA-PEG-folate conjugate, J. Drug Target. 16 (5) (2008) 415–423.
[40] D. Hu, Z. Sheng, S. Fang, Y. Wang, D. Gao, P. Zhang, P. Gong, Y. Ma, L. Cai, Folate receptor-targeting gold nanoclusters as fluorescence enzyme mimetic nanoprobes for tumor molecular colocalization diagnosis, Theranostics 4 (2) (2014) 142–153.
[41] U.B. Sleytr, M. Sara, S. Küpcü, P. Messner, Structural and chemical characterization of S-layers of selected strains of Bacillus stearothermophilus and Desulfotomaculum nigrificans, Arch. Microbiol. 146 (1986) 1–19.
[42] Y. Song, Y. Chen, L. Feng, J. Ren, X. Qu, Selective and quantitative cancer cell detection using target-directed functionalized graphene and its synergetic peroxidase-like activity, Chem. Commun. 47 (2011) 4436–4438.
[43] M. Picher, S. Küpcü, C.J. Huang, J. Dostalek, D. Pum, U.B. Sleytr, P. Ertl, Nanobiotechnology advanced antifouling surfaces for the continuous electrochemical monitoring of glucose in whole blood using a lab-on-a-chip, Lab Chip 13 (2013) 1780–1789.
[44] M. Sara, U.B. Sleytr, Crystalline bacterial cell surface layers (S-layers): from cell structure to biomimetics, Prog. Biophys. Mol. Biol. 65 (1996) 83–111.
[45] A. Schrems, V.D. Larisch, C. Stanetty, K. Dutter, S. Damiati, U.B. Sleytr, B. Schuster, Liposome fusion on proteinaceous S-layer lattices triggered via β-diketone ligand-europium(III) complex formation, Soft Matter 7 (2011) 5514–5518.
[46] S. Kim, T. Fujii, Efficient analysis of a small number of cancer cells at the single-cell level using an electroactive double-well array, Lab Chip 16 (2016) 2440–2449.
[47] E.S. Györvary, O. Stein, D. Pum, U.B. Sleytr, Self-assembly and recrystallization of bacterial S-layer proteins at silicon supports imaged in real time by atomic force microscopy, J. Microsc. 212 (2003) 300–306.
[48] M. Tarantola, A. Marel, E. Sunnick, H. Adam, J. Wegener, A. Janshoff, Dynamics of human cancer cell lines monitored by electrical and acoustic fluctuation analysis, Integr. Biol. 2 (2010) 139–150.
[49] X. Li, S. Song, Q. Shuai, Y. Pei, T. Aastrup, Y. Pei, Z. Pei, Real-time and label-free analysis of binding thermodynamics of carbohydrate-protein interactions on unfixed cancer cell surfaces using a QCM biosensor, Sci. Rep. 5 (2015) 14066.
[50] D. Sharma, Y. Lim, Y. Lee, H. Shin, Glucose sensor based on redox-cycling between selectively modified and unmodified combs of carbon interdigitated array nanoelectrodes, Anal. Chim. Acta 889 (2015) 194–202.